Journal of Superconductivity and Novel Magnetism (2020) 33:1249–1256
https://doi.org/10.1007/s10948-020-05451-z

LETTER

Structural, Optical, and Magnetic Properties of the New (1-x) $Bi_{0.5}Na_{0.5}TiO_3$ + $xMgCoO_{3-\delta}$ Solid Solution System

Dang Duc Dung [1] · Nguyen The Hung [1,2]

Received: 22 December 2019 / Accepted: 3 February 2020 / Published online: 13 February 2020
© Springer Science+Business Media, LLC, part of Springer Nature 2020

Abstract

A new (1-*x*)$Bi_{0.5}Na_{0.5}TiO_3$ + *x*$MgCoO_{3-\delta}$ solid solution system was synthesized using the simple sol–gel method. The structure that was investigated via X-ray diffraction and Raman scattering analysis indicated that the $MgCoO_{3-\delta}$ materials were highly soluble into the host $Bi_{0.5}Na_{0.5}TiO_3$ crystals. The random incorporation of Mg and Co cations into the host crystal of the $Bi_{0.5}Na_{0.5}TiO_3$ materials reduced the optical band gap energy and induced a complex magnetic behavior as a function of $MgCoO_{3-\delta}$ concentration solute in the host matrix. The optical band gap energy values decreased from 3.05 eV for pure $Bi_{0.5}Na_{0.5}TiO_3$ materials to 2.22 eV with 9 mol% $MgCoO_{3-\delta}$ solution for the $Bi_{0.5}Na_{0.5}TiO_3$ compounds. A weak ferromagnetic property with strongly induced diamagnetism was obtained at room temperature for the pure $Bi_{0.5}Na_{0.5}TiO_3$ materials, whereas ferromagnetic properties were observed for the $MgCoO_{3-\delta}$-modified $Bi_{0.5}Na_{0.5}TiO_3$ compounds. The addition of paramagnetic and/or antiferromagnetic-like behavior was obtained for the $MgCoO_{3-\delta}$ solid solution with over 5 mol% in the host $Bi_{0.5}Na_{0.5}TiO_3$ materials. This work contributes to the current understanding of the interaction of transition metal cations in the host crystal ABO_3 perovskite of lead-free ferroelectric materials due to the co-modification of *A* and *B* sites.

Keywords $Bi_{0.5}Na_{0.5}TiO_3$ · $MgCoO_{3-\delta}$ · Lead-free ferroelectric · Ferromagnetism · Sol-gel

1 Introduction

Integration of the ferromagnetic property into lead-free ferroelectric materials provides a possibility of developing new material functions because their components can be adapted for two required parameters that are sacrificed in new general electronic device applications. Moreover, they are eco-friendly with the human body and the environment. Among lead-free ferroelectric materials, $Bi_{0.5}Na_{0.5}TiO_3$ is one of the important host materials with recently advanced electrical field-induced strain properties in comparison with $Pb(Zr,Ti)O_3$-based materials [1]. $Bi_{0.5}Na_{0.5}TiO_3$ materials were first synthesized by Smolenskii et al. in 1960; in their study, $Bi_{0.5}Na_{0.5}TiO_3$ materials exhibited large remnant polarization (P_r = 38 μC/cm^2), high Curie temperature (T_C = 320 °C), and high piezoelectric coefficient (d_{33} = 74.0–94.8 pC/N) [2–5]. The pure $Bi_{0.5}Na_{0.5}TiO_3$ materials displayed weak ferromagnetism primarily due to self-defects and/or surface defects, such as Ti and Na vacancies [6, 7]. The theoretical prediction is that Ti and Na vacancies display larger magnetic moments than those of Bi or O vacancies [8]. In addition, the first principle theoretical calculation predicts that the Na surface or grain boundary also exhibits a large magnetic moment [6, 8]. However, the magnetization of pure $Bi_{0.5}Na_{0.5}TiO_3$ materials is slightly influenced by the diamagnetic signal from the empty orbital of Ti^{4+} [7, 9–11]. Therefore, searching for high-magnetization ferromagnetic materials and suppressing the diamagnetic properties of lead-free ferroelectric $Bi_{0.5}Na_{0.5}TiO_3$ materials are the next challenges in establishing the required transfer material for real electronic device applications.

The magnetic properties of lead-free ferroelectric $Bi_{0.5}Na_{0.5}TiO_3$ materials have been overcome recently by using various fabrication methods, such as doping or solid solution method [7, 9–17]. However, the origin of room temperature ferromagnetism in transition metals contained in lead-free ferroelectric $Bi_{0.5}Na_{0.5}TiO_3$ materials remains

✉ Dang Duc Dung
dung.dangduc@hust.edu.vn

[1] Department of General Physics, School of Engineering Physics, Ha Noi University of Science and Technology, 1 Dai Co Viet road, Ha Noi, Vietnam

[2] Faculty of Basic - Fundamental Sciences, Viet Nam Maritime University, 484 Lach Tray street, Hai Phong, Vietnam

unclear. Therefore, understanding the origin of ferromagnetic ordering in lead-free ferroelectric materials is crucial and guides the search and development of high-performance materials. Wang et al. obtained ferromagnetic properties in lead-free ferroelectric $Bi_{0.5}Na_{0.5}TiO_3$ by using transition metals Fe and Co as impurities, but the ferromagnetic ordering was attained in a different way [9, 10]. The ferromagnetic property in Fe-doped $Bi_{0.5}Na_{0.5}TiO_3$ materials was explanted via the interaction of Fe cations through O vacancies (□), such Fe^{3+}-□-Fe^{3+}, where the ferromagnetic ordering in Co-doped $Bi_{0.5}Na_{0.5}TiO_3$ materials resulted from magnetic clusters of Co that were formed during sample fabrication [9, 10]. The interaction between magnetic ions through O vacancies resulting from the ferromagnetic ordering were also applied to explant the ferromagnetism in Mn-doped $Bi_{0.5}Na_{0.5}TiO_3$ materials, where the possible interaction of $Mn^{2+/3+}$-□-$Mn^{2+/3+}$ favors ferromagnetism [11]. Recently, we proposed that the ferromagnetism in Fe- and Co-doped lead-free ferroelectric $Bi_{0.5}Na_{0.5}TiO_3$ materials is possibly an intrinsic phenomenon in which the possible enhancement magnetization is contributed by the magnetic property of Ti cations due to charge transfer [12, 13]. In addition, Thanh et al. reported that O vacancies possibly enhance the magnetic performance of $Bi_{0.5}Na_{0.5}TiO_3$ materials [7]. However, due to the limitation in the number of transition metals in the element periodic table, studies on the current development of ferromagnetic properties in lead-free ferroelectric materials are limited. Owing to the good solid solution of $Bi_{0.5}Na_{0.5}TiO_3$ with various impurity phase carriers, we recently developed a new method to inject ferromagnetic properties in lead-free ferroelectric $Bi_{0.5}Na_{0.5}TiO_3$ materials by using a solid solution with various types of materials, such as ilmenite-type (e.g., $MnTiO_3$ and $NiTiO_3$) and perovskite-type (e.g., $SrFeO_{3-\delta}$ and $BaMnO_{3-\delta}$) materials [14–17]. For an ilmenite-type solid solution in $Bi_{0.5}Na_{0.5}TiO_3$ materials, the magnetic properties of $Bi_{0.5}Na_{0.5}TiO_3$ materials are enhanced, which originate not only from the interaction of transition metals but also from magnetic Na vacancies [14, 15]. For a perovskite-type solid solution in $Bi_{0.5}Na_{0.5}TiO_3$ materials, the magnetic properties of $Bi_{0.5}Na_{0.5}TiO_3$ materials are advanced via the contribution of the magnetic direction of Na vacancies or indirection of O vacancies due to the multi-substitution of alkali-earth at the (Bi^{3+}, Na^{+})-site [16, 17]. Notably, O vacancies have a narrow magnetic moment but promote the reduction of Ti valence from Ti^{4+} to Ti^{3+}, which enhances the magnetic moment [18, 19]. Recently, Mg-based alkali-earth-modified $Bi_{0.5}Na_{0.5}TiO_3$ materials (e.g., $MgMnO_{3-\delta}$ and $MgFeO_{3-\delta}$) have been found to greatly enhance magnetic properties compared with single transition metal doping into host $Bi_{0.5}Na_{0.5}TiO_3$ materials [20, 21]. These interesting results originated from the complex random incorporation of Mg cations in *A*- and *B*- sites, where Mg cations are the possible substitute for all cations in the host lattice of $Bi_{0.5}Na_{0.5}TiO_3$ [20, 21]. Recently, Dung et al. reported that Co cations incorporated into the Ti site display a small magnetic moment, and the magnetic signal is strongly influenced by the diamagnetic component of the empty state of Ti^{4+} cations [12]. Therefore, we expect that the co-modification of Mg and Co cations possibly enhances the magnetic performance of lead-free ferroelectric materials by using $MgCoO_{3-\delta}$ as impurities for the solid solution in the host $Bi_{0.5}Na_{0.5}TiO_3$ crystal.

In this work, a new solid solution of the $MgCoO_{3-\delta}$ and $Bi_{0.5}Na_{0.5}TiO_3$ system was fabricated with the sol–gel method. The Mg and Co cations were successfully incorporated into the host lattice of the $Bi_{0.5}Na_{0.5}TiO_3$ crystal, resulting in the reduction of optical band gap values and induced complex magnetic behavior.

2 Experimental

The $(1\text{-}x)Bi_{0.5}Na_{0.5}TiO_3 + xMgCoO_{3-\delta}$ (named as BNT pure and BNT-x$MgCoO_{3-\delta}$, $x = 0.5$, 1, 3, 5, 7, and 9 mol%) solid solution system was fabricated with the sol–gel technique. The initial chemical source included $Bi(NO_3)_3{\cdot}6H_2O$, $NaNO_3$, $C_{12}H_{28}O_4Ti$, $Mg(NO_3)_2$, and $Co(NO_3)_2{\cdot}6H_2O$. Acetyl acetone ($CH_3COCH_2COCH_3$) and acetic acid (CH_3COOH) were used as the ligand for avoiding the hydroxyl of cations during sol creation. The ligand solution was prepared by mixing deionized water with acetic acid solution at a fraction volume of 5:1. First, $Bi(NO_3)_3{\cdot}6H_2O$ was weighed and distinguished in the solution by magnetic stirring until transparency. Second, $NaNO_3$, $Mg(NO_3)_2$, and $Co(NO_3)_3.9H_2O$ were weighed to be added and distinguished in the solution. To avoid the hydroxyl of Ti^{4+} cations, acetyl acetone was added dropwise in the solution before the $C_{12}H_{28}O_4Ti$ solution. The final solutions were continuously magnetically stirred at approximately 3–4 h before drying in an oven at approximately 100 °C to form dry gel. The dry gel was routed to the grid before thermal annealing under 900 °C for 3 h in air to form sample powder. The appearance of the chemical element in the final compounds of the sample powder was measured via energy dispersive X-ray spectroscopy (EDX). The concentration of each element in the compound further confirmed the chemical composition via electron probe microanalysis (EPMA). Sodium is a light element that is easy to evaporate during gelling and sintering and thus has a non-stoichiometric composition [14–17]. Thus, the sodium chemical element was given extra weight from the initial $NaNO_3$ source [14–17]. The EPMA results confirmed that the $NaNO_3$ source was weighed to extra at approximately 50 mol% and was deficient for the loss of Na in the compound. The crystal structural symmetry of the samples was studied through X-ray diffraction (XRD). The typical vibration modes of the samples were measured using Raman scattering. The optical absorbance and photoluminescence (PL) properties of the samples

were determined using ultraviolet-visible spectroscopy (UV–Vis) and PL, respectively. The magnetic properties of the samples were measured with a vibrating sample magnetometer. All measurements were performed at room temperature.

3 Results and Discussions

Figure 1a and b show the EDX spectra of pure $Bi_{0.5}Na_{0.5}TiO_3$ materials and $MgCoO_{3-\delta}$-modified $Bi_{0.5}Na_{0.5}TiO_3$ materials with 5 mol% $MgCoO_{3-\delta}$, respectively. The inset of each figure displays the selected area for EDX chemical detection. The results clearly indicate that the pure $Bi_{0.5}Na_{0.5}TiO_3$ materials contained typical peaks of Bi, Na, Ti, and O. The addition of extra Mg and Co peaks in the EDX spectra, as shown in Fig. 1b, provided solid evidence for the presentation of impurities Mg and Co, which were embedded in our samples. The concentration of each element in pure $Bi_{0.5}Na_{0.5}TiO_3$ and $MgCoO_{3-\delta}$-modified $Bi_{0.5}Na_{0.5}TiO_3$ materials was further confirmed via EPMA. The impurities Mg and Co cations were well detected in the doped $Bi_{0.5}Na_{0.5}TiO_3$ samples.

Figure 2a shows the XRD of pure $Bi_{0.5}Na_{0.5}TiO_3$ and $MgCoO_{3-\delta}$-modified $Bi_{0.5}Na_{0.5}TiO_3$ materials with various $MgCoO_{3-\delta}$ concentrations. Based on the peak position and in relation to peak intensity, the results reveal that the samples exhibited a perovskite structure with rhombohedral symmetry.

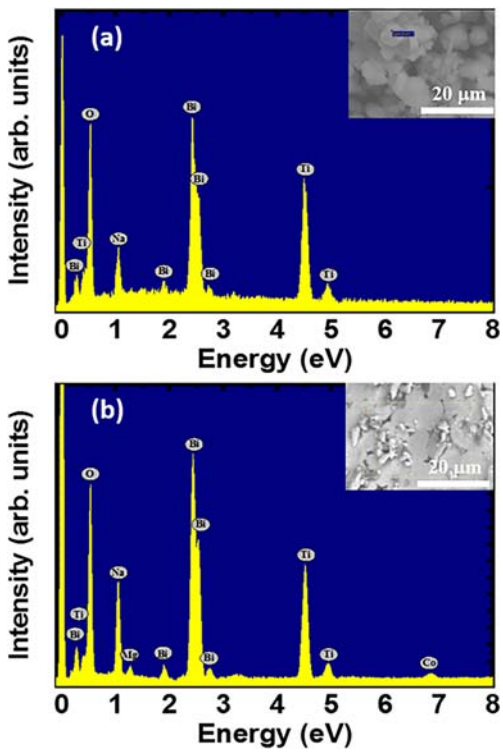

Fig. 1 EDX spectra of **a** pure $Bi_{0.5}Na_{0.5}TiO_3$ materials and **b** $MgCoO_{3-\delta}$-modified $Bi_{0.5}Na_{0.5}TiO_3$ materials with 5 mol% $MgCoO_{3-\delta}$. The inset of each figure shows the selection of the area for chemical composition indexing

The peaks of the trade phase and/or phase separation could not be detected from the XRD resolution. The results indicate that the possible $MgCoO_{3-\delta}$ phase solute solution in the host $Bi_{0.5}Na_{0.5}TiO_3$ resulted in the random incorporation of Mg and Co cations into the host crystal of $Bi_{0.5}Na_{0.5}TiO_3$ materials. The influence of Mg and Co cations on the lattice host of the $Bi_{0.5}Na_{0.5}TiO_3$ crystal is shown in Fig. 2b, where the 2θ diffraction angle is magnified in the range of 31.0 ° to 34.0 °. The couple (012)/(110) peaks overlapped, making it difficult to compare the influence of Mg and Co on the host lattice. Each peak was distinguished via Lorentz fitting with *r*-square over 0.99. The results indicate that the peak position shifted to a low diffraction angle, providing solid evidence of the random incorporation of Mg and Co cations into the host lattice that resulted in the expansion of the lattice parameter. The distortion of the lattice parameter of the host $Bi_{0.5}Na_{0.5}TiO_3$ materials via Mg and Co cation incorporation was possibly explanted by considering the radius difference between the host and impurity cations. According to Shannon's report, the radii of host cation Bi^{3+} (in coordination with VIII), Na^{+} (in coordination with XII), and Ti^{4+} (in coordination with IV) are 1.17, 1.39, and 0.605 Å, respectively [22]. The radius of Mg^{2+} cations is 0.89 and 0.72 Å for coordination with XII and VI, respectively. Therefore, if the Mg^{2+} cations are randomly incorporated with the Bi^{3+} or Na^{+} site, they would result in a compressed lattice parameter. However, if the Mg^{2+} cations are substituted for the Ti^{4+} site, the lattice parameter would be expanded. Similarly, the Co cations were also complex in the incorporation with the host lattice caused by the possible presence of the multivalence and dependent spin state. In a high spin state, Co^{2+}, Co^{3+}, and Co^{4+} cations have a radius of 0.745, 0.61, and 0.53 Å, respectively, with the coordination of VI [22]. In a low spin state, Co^{2+} and Co^{3+} cations have a radius of 0.65 and 0.545 Å, respectively, with the same coordination [22]. Therefore, if the Co cations existed in a low spin state in the host crystal of $Bi_{0.5}Na_{0.5}TiO_3$ materials, then the lattice parameter would possibly be expanded for the Co cations present with the valence state of Co^{2+}. Meanwhile, Co^{3+} cations result in a compressed lattice parameter when substituted for the Ti^{4+} site. The trend is similar to that of Co^{2+}, Co^{3+}, and Co^{4+} cations in a high spin state substituted for the Ti^{4+} site. The Co^{2+} and Co^{3+} cations expanded the lattice parameter, whereas the Co^{4+} cations reduced the lattice parameter. However, the phenomenon became complex when Mg that substituted for the *A*-site and Mg^{2+} that substituted for Bi^{3+} created O vacancies. Mg^{2+} cooperated with the Na^{+} site where the generated Na vacancies are. Similarly, Co^{2+} and Co^{3+} cations that substituted for the Ti^{4+} site created O vacancies, which were required for the balance charge of samples. The O vacancies reduced the lattice parameter because the radii of these O vacancies were smaller than that of anion O and helped decrease the valence charge of Ti and Co; for example, Ti^{4+} was changed to Ti^{3+} and Co^{3+} was reduced to

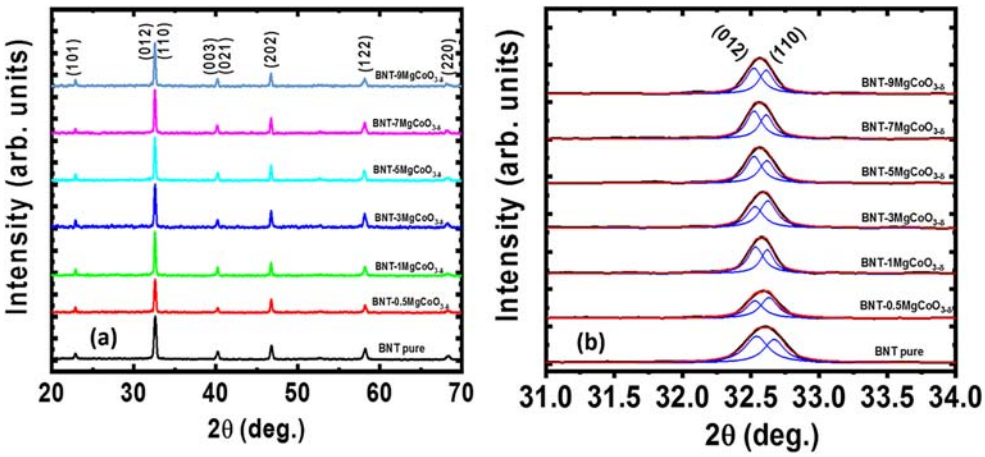

Fig. 2 X-ray diffraction of pure $Bi_{0.5}Na_{0.5}TiO_3$ and $MgCoO_{3-\delta}$-modified $Bi_{0.5}Na_{0.5}TiO_3$ materials with various of $MgCoO_{3-\delta}$ amounts as the solid solution in a diffraction angle 2θ range of **a** 20° to 70° and **b** magnified 2θ from 31.0 ° to 34.0 °

Co^{2+} [18, 22–24]. However, this main contribution requires further investigation. The distortion of the lattice parameter of $Bi_{0.5}Na_{0.5}TiO_3$ materials provided solid evidence on the random incorporation of Mg and Co cations into the host lattice to form a solid solution.

Figure 3a shows the Raman scattering of $Bi_{0.5}Na_{0.5}TiO_3$ and $MgCoO_{3-\delta}$-modified $Bi_{0.5}Na_{0.5}TiO_3$ materials with various $MgCoO_{3-\delta}$ amounts. As the solute solution of the $MgCoO_{3-\delta}$ phase in the host lattice of $Bi_{0.5}Na_{0.5}TiO_3$ crystals, similar Raman scattering curves were obtained for pure $Bi_{0.5}Na_{0.5}TiO_3$ and $MgCoO_{3-\delta}$-modified $Bi_{0.5}Na_{0.5}TiO_3$ samples. The random distribution of Bi and Na cations at the *A* site of the perovskite structure $Bi_{0.5}Na_{0.5}TiO_3$ materials resulted in a broad band Raman scattering observation. Based on the Raman scattering spectra, we devised three main regions, namely, approximately 300–450, 450–670, and 670–900 cm^{-1}. Experimentation was combined with theoretical investigation to study the Raman scattering vibration modes of $Bi_{0.5}Na_{0.5}TiO_3$ materials. The results showed that the frequency modes were within the range 109–134 cm^{-1}, and Na–O and $[TiO_6]$ vibrations were assigned in the frequency range of 155–187 and 246–401 cm^{-1}, respectively. High frequencies in the range of 413–826 cm^{-1} were dominated by vibrations of the O atoms [25]. The modes in the frequency of 150–450 cm^{-1} were related to Ti–O vibrations, and the bands between 450 and 700 cm^{-1} were related to $[TiO_6]$ vibrations, which are the breathing and stretching modes of the O octahedra [26]. The TO_3 mode situated at approximately 541 cm^{-1} may be due to the O–Ti–O stretching symmetric vibration of the octahedral $[TiO_6]$ cluster, and the LO3 modes at 813 cm^{-1} were due to the presence of the sites within the rhombohedral lattice containing the octahedral distorted $[TiO_6]$ clusters [27, 28]. High-frequency bands, such as 486, 526, and 583 cm^{-1}, were dominated by vibration involving mainly O displacements [29]. The Raman peaks of pure $Bi_{0.5}Na_{0.5}TiO_3$ and $MgCoO_{3-\delta}$-modified $Bi_{0.5}Na_{0.5}TiO_3$ samples overlapped. Therefore, comparing the changes in vibration modes due to the random incorporation of Mg and Co cations into the host crystal was difficult. We used Lorentz fitting for each sample to distinguish each vibration mode. The correction of each fitting result was consistent with the *r*-square values over 0.99. The fitting results for pure $Bi_{0.5}Na_{0.5}TiO_3$ and $MgCoO_{3-\delta}$-modified $Bi_{0.5}Na_{0.5}TiO_3$ samples with 1 mol%, 5 mol%, and 9 mol% $MgCoO_{3-\delta}$ are shown in Fig. 3b. The Raman vibration modes were estimated to be approximately nine vibration modes in the observation of active Raman scattering. The results are consistent with the theoretical prediction of Niranjan et al. [25]. The active Raman modes at

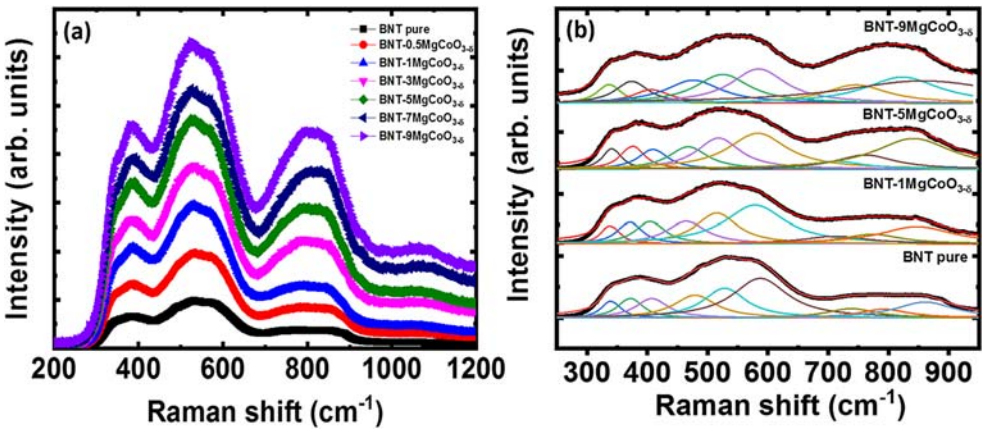

Fig. 3 **a** Raman scattering spectra of pure $Bi_{0.5}Na_{0.5}TiO_3$ and $MgCoO_{3-\delta}$-modified $Bi_{0.5}Na_{0.5}TiO_3$ materials with various $MgCoO_{3-\delta}$ amounts as the solid solution. **b** Devolution Raman scattering peaks for pure $Bi_{0.5}Na_{0.5}TiO_3$ and $MgCoO_{3-\delta}$-modified $Bi_{0.5}Na_{0.5}TiO_3$ materials with 1, 5, and 9 mol% $MgCoO_{3-\delta}$ amounts as the solid solution

approximately 530 cm^{-1} shifted to a low frequency for the low $MgCoO_{3-\delta}$ solute solution and shifted back to a high frequency when the $MgCoO_{3-\delta}$ concentration in the solute solution was increased. These results suggest that Co and Mg modified the Ti site and/or resulted from distorted lattice parameters, thereby affecting the Ti–O or TiO_6 vibration. In addition, the broad band in the vibration peaks at a high frequency in the range of 670–900 cm^{-1} further suggested enlarged O vacancies. The combination of XRD and Raman scattering analysis of the influence of $MgCoO_{3-\delta}$-modified $Bi_{0.5}Na_{0.5}TiO_3$ samples indicated that the $MgCoO_{3-\delta}$ materials were highly soluble in the $Bi_{0.5}Na_{0.5}TiO_3$ crystal, resulting in the random distribution of Mg and Co cations into the host crystal during the formation of the solid solution.

Figure 4a shows the absorbance spectroscopy of pure $Bi_{0.5}Na_{0.5}TiO_3$ and $MgCoO_{3-\delta}$-modified $Bi_{0.5}Na_{0.5}TiO_3$ samples with various $MgCoO_{3-\delta}$ amounts. The pure $Bi_{0.5}Na_{0.5}TiO_3$ materials exhibited a single absorbance edge at approximately 450 nm and had a light tail. The single edge absorbance of pure $Bi_{0.5}Na_{0.5}TiO_3$ materials was well understood via theoretical prediction for the electronic band structure of their materials, where the direction transition was dominant for optical transition [30, 31]. The light tail along the wavelength of around 600 nm in the absorbance spectra of pure $Bi_{0.5}Na_{0.5}TiO_3$ possibly originated from the intrinsic defect and/or surface effect, where the defects reduced the optical band gap values [6, 8, 12]. The addition of $MgCoO_{3-\delta}$ as a solid solution into the host $Bi_{0.5}Na_{0.5}TiO_3$ materials strongly modified the electronic band structure. The optical absorbance spectra became complex with multi-shoulders. The absorbance edge of $MgCoO_{3-\delta}$-modified $Bi_{0.5}Na_{0.5}TiO_3$ materials was not sharp compared with the absorbance spectra of pure $Bi_{0.5}Na_{0.5}TiO_3$ materials and tended to shift to a high wavelength. In addition, the multi-absorbance peaks were clearly presented. The appearance of multi-defects in the electronic band structure of $Bi_{0.5}Na_{0.5}TiO_3$ materials via defects made the optical transition of electrons possible, resulting in the reduction of the optical band gap. The typical absorption in the absorbance spectra of $MgCoO_{3-\delta}$-modified $Bi_{0.5}Na_{0.5}TiO_3$ materials has been suggested for the typical valence state of Co and Mg cations [12, 20, 21]. The optical band gap values of the pure $Bi_{0.5}Na_{0.5}TiO_3$ and $MgCoO_{3-\delta}$-modified $Bi_{0.5}Na_{0.5}TiO_3$ samples with various $MgCoO_{3-\delta}$ amounts were estimated using the Wood–Tauc method [32]. The $(\alpha h\nu)^2$ values were plotted as a function of absorbance photon energy ($h\nu$) for the pure $Bi_{0.5}Na_{0.5}TiO_3$ and $MgCoO_{3-\delta}$-modified $Bi_{0.5}Na_{0.5}TiO_3$ samples, where α is the absorbance coefficient, h is the Plank constant, and ν is the frequency of absorbance wavelength photon, as shown in Fig. 4b. The optical band gap values (E_g) were estimated from a linear proportion. E_g of the pure $Bi_{0.5}Na_{0.5}TiO_3$ samples was estimated to be approximately 3.05 eV. These results are consistent with recently reported optical band gap energy values for pure $Bi_{0.5}Na_{0.5}TiO_3$ materials [33]. The addition of $MgCoO_{3-\delta}$ into the host $Bi_{0.5}Na_{0.5}TiO_3$ materials as a solid solution reduced the optical band gap energy up to 2.22 eV for 9 mol% $MgCoO_{3-\delta}$ solute. The details of the E_g values as a function of $MgCoO_{3-\delta}$ concentration are plotted in the inset of Fig. 4b. At this moment, the origin of the reduction in optical band gap values remained unclear and complex due to various effects, which possibly tuned the effectiveness of optical band gap energy. The reduction in E_g values was possibly related to two main reasons, namely, occurrence of a new local state in the middle electronic band structure and O vacancies located below the conduction band. The new local state of impurities, such as Co and Mg, was also complicated because of the possible presence of multivalence Co cations and the multi-substitution of Mg cations in *A*- and *B*-sites in the perovskite structure. The possible valence state of several cations was also affected by the optical band gap, such as reduction in valence state Ti^{4+} to Ti^{3+} or Co^{3+} to Co^{2+} because of O vacancies, which also induced the new local state of impurities

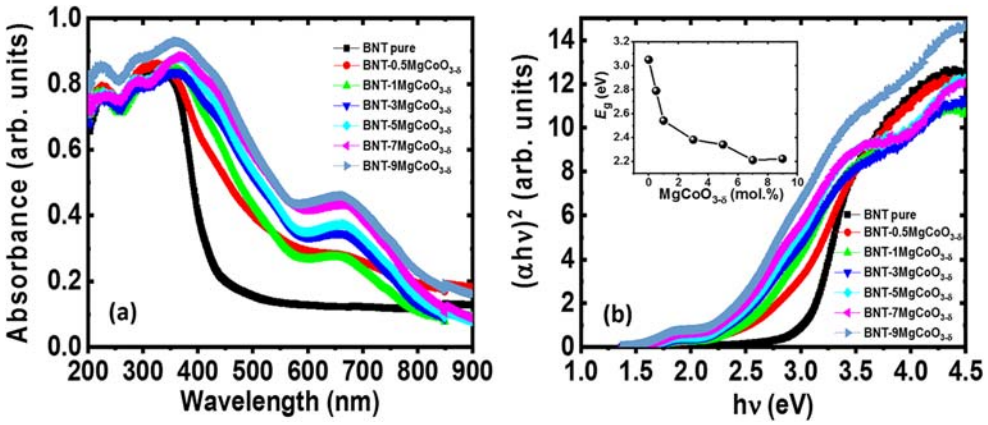

Fig. 4 **a** Absorbance spectra of pure $Bi_{0.5}Na_{0.5}TiO_3$ and $MgCoO_{3-\delta}$-modified $Bi_{0.5}Na_{0.5}TiO_3$ materials with various $MgCoO_{3-\delta}$ amounts as the solid solution. **b** Plot of $(\alpha h\nu)^2$ as a function of photon energy ($h\nu$) for pure $Bi_{0.5}Na_{0.5}TiO_3$ and $MgCoO_{3-\delta}$-modified $Bi_{0.5}Na_{0.5}TiO_3$ materials with various $MgCoO_{3-\delta}$ amounts as the solid solution. The inset of Fig. 4(b) shows the E_g values as a function of the $MgCoO_{3-\delta}$ concentration solute in the $Bi_{0.5}Na_{0.5}TiO_3$ materials

[18, 22–24]. Moreover, the possible creation of O vacancies resulted from the substitution of $Co^{2+/3+}$ for Ti^{4+} or Mg^{2+} for Bi^{3+}/Ti^{4+} and generated Na vacancies from the incorporation of Mg^{2+} for the Na^{+} site, resulting in a new local state. The electronic band structure of $Bi_{0.5}Na_{0.5}TiO_3$ via random incorporation of Mg and Co cations needs to be further investigated via theoretical prediction to reveal the clear contribution of their cations to the total electronic structure. However, in this work, the shifted absorbance edge and the induced complex absorbance peaks in the $Bi_{0.5}Na_{0.5}TiO_3$ materials via $MgCoO_{3-\delta}$ addition provided further evidence on the random incorporation of Mg and Co cations into the host crystal of $Bi_{0.5}Na_{0.5}TiO_3$ materials during the formation of the solid solution.

Figure 5 shows the photoluminescence (PL) spectra of pure $Bi_{0.5}Na_{0.5}TiO_3$ and $MgCoO_{3-\delta}$-modified $Bi_{0.5}Na_{0.5}TiO_3$ materials as a solid solution with various $MgCoO_{3-\delta}$ amounts. The PL spectra can be divided into two major ranges, namely, 480–500 and 720–100 nm. The shoulder PL range of 600–720 was also obtained. The low PL wavelength range was magnified in the range of 480–500 nm and shown in the inset of Fig. 5. The low PL range from 480 nm to 500 nm was strongly related to the surface defect where the unsaturated bonding pair existed for cations on the surface [20, 34]. The added amounts of $MgCoO_{3-\delta}$ to the $Bi_{0.5}Na_{0.5}TiO_3$ materials resulted in suppressed PL on the surface, as shown in the inset of Fig. 5, which possibly originated from the charge secondary absorbance of the PL of the surface self-defects. The PL of the shoulder around 600–720 nm was strongly related to the absorbance of defects, which is consistent with the absorbance spectra. However, a strong PL intensity was obtained for a high wavelength from 720 nm to around 1000 nm. At this moment, we could not correctly determine the origin of PL in their wavelength range. However, based on the low energy of photon PL, we speculate that the results are mostly related to the Mg–Co complex transition and/or the transition of O vacancies in our samples.

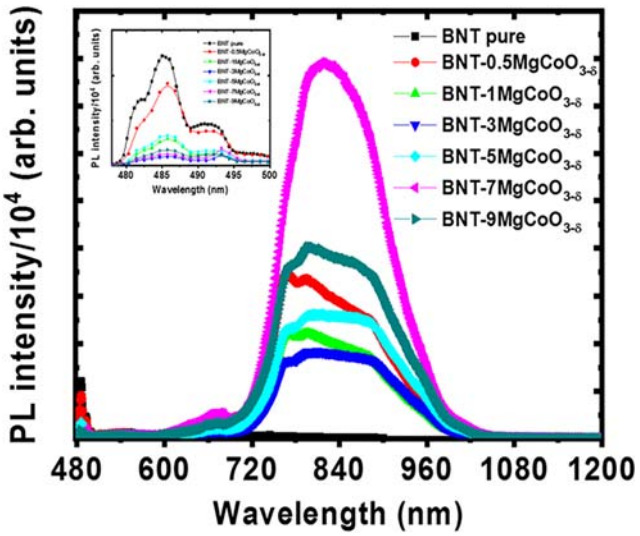

Fig. 5 Photoluminescence spectra of pure $Bi_{0.5}Na_{0.5}TiO_3$ and $MgCoO_{3-\delta}$-modified $Bi_{0.5}Na_{0.5}TiO_3$ materials with various $MgCoO_{3-\delta}$ amounts as the solid solution. The inset of Fig. 5 shows the magnification of photoluminescence in a wavelength range of 480–500 nm for pure $Bi_{0.5}Na_{0.5}TiO_3$ and $MgCoO_{3-\delta}$-modified $Bi_{0.5}Na_{0.5}TiO_3$ materials with various $MgCoO_{3-\delta}$ amounts as the solid solution

Figure 6 a–g show magnetization as a function of applied external magnetic field (M-H) at room temperature for pure $Bi_{0.5}Na_{0.5}TiO_3$ materials and $MgCoO_{3-\delta}$-modified $Bi_{0.5}Na_{0.5}TiO_3$ materials with various $MgCoO_{3-\delta}$ amounts as a solid solution. The results clearly indicated that the solute of $MgCoO_{3-\delta}$ into the host $Bi_{0.5}Na_{0.5}TiO_3$ materials strongly induced a complex magnetic behavior. The concentration of $MgCoO_{3-\delta}$ was an important parameter for tuning the magnetic properties of the $Bi_{0.5}Na_{0.5}TiO_3$ materials. The pure $Bi_{0.5}Na_{0.5}TiO_3$ materials exhibited a combination of diamagnetism and weak ferromagnetism. The anti-S-shape in the M–H curves is shown in Fig. 6a. The clear evidence of the weak ferromagnetism of the pure $Bi_{0.5}Na_{0.5}TiO_3$ materials is shown in the inset of Fig. 6a, after the substrate of the diamagnetic component by the typical ferromagnetic M–H hysteresis loop. The origin of the weak ferromagnetism in pure $Bi_{0.5}Na_{0.5}TiO_3$ materials is well understood via theoretical prediction and experimental observation; intrinsic defects and/or surface effects, such as Na and Ti vacancies, exist during sample fabrication [6–11]. The diamagnetic property of pure $Bi_{0.5}Na_{0.5}TiO_3$ materials is mostly related to the empty state of Ti^{4+} cations [7]. In the current study, the addition of $MgCoO_{3-\delta}$ to the host $Bi_{0.5}Na_{0.5}TiO_3$ materials as a solid solution suppressed the diamagnetic component and the instance of complex magnetic properties, as shown in Fig. 6 b–f, where the anti-S-shape in the M–H curves changed to an S-shape. Further addition of $MgCoO_{3-\delta}$ resulted in unsaturation of the magnetic moment with the applied external magnetic field, as shown in Fig. 6g. The origin of the complex magnetic properties of $MgCoO_{3-\delta}$-modified $Bi_{0.5}Na_{0.5}TiO_3$ materials was not well understood at this moment due to the various possible magnetic sources, which possibly induced the magnetic moment of the samples. First, the possibly induced $Co^{2+/3+}$ interaction through the O vacancies, $Co^{2+/3+}$-□-$Co^{2+/3+}$, was given the ferromagnetic ordering. However, we recently reported that possible Co cations are favored in a low-spin states; they display a low magnetic moment and possible charge transfer to Ti^{4+} cations, resulting in a strong, induced magnetic moment via the reduction of the valence state of Ti^{4+} to $Ti^{(4-\delta)+}$ [12]. Therefore, we suggest that the other possible sources of $Co^{2+/3+}$-□-$Ti^{(4-\delta)+}$ are an important interaction part for the induced magnetic moment. In addition, the random incorporation of Mg cations in *A*- and *B*-sites possibly created the Na and O vacancies [20, 21]. The Na vacancies in $Bi_{0.5}Na_{0.5}TiO_3$ materials are the well-known origin of ferromagnetism [6, 8]. Moreover, the O vacancies promoted the reduction of the valence state of Ti^{4+}, and the $Co^{3+/4+}$ cations were an important

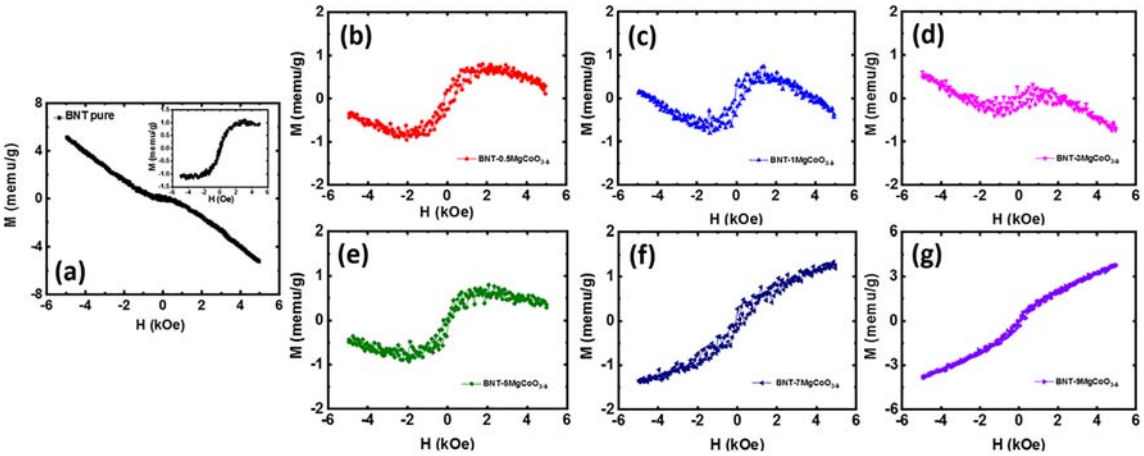

Fig. 6 Magnetic moment as a function of applied external magnetic field for **a** pure $Bi_{0.5}Na_{0.5}TiO_3$ and **b**–**g** $MgCoO_{3-\delta}$-modified $Bi_{0.5}Na_{0.5}TiO_3$ materials with 0.5, 1, 3, 5, 7, and 9 mol% of $MgCoO_{3-\delta}$ as the solid solution. The inset of Fig. 6a shows the hysteresis loop of pure $Bi_{0.5}Na_{0.5}TiO_3$ materials after the substrate in the diamagnetic component

source for the ferromagnetic material [18, 22–24]. The ferromagnetism in $Bi_{0.5}Na_{0.5}TiO_3$ materials needs an in-depth investigation, such as by first principle theoretical calculation. Finally, the observation of the unsaturation of magnetic moment with the applied low-strength external magnetic field, as shown in Fig. 6g, was consistent with the polarization boundary model where antiferromagnetic-like materials are favored for $Co^{2+/3+}$-□-$Co^{2+/3+}$ versus $Co^{2+/3+}$-□-$Co^{2+/3+}$ interaction. In addition, the isolate of magnetic cations, such as $Co^{2+/3+/4+}$, $Ti^{(4-\delta)+}$, or Na and Ti vacancies, exhibited a paramagnetic behavior, resulting in the unsaturation of the magnetic moment with the applied external magnetic field. In other words, the complex magnetic behavior of the $MgCoO_{3-\delta}$-modified $Bi_{0.5}Na_{0.5}TiO_3$ materials was not well understood at this moment, but a typical ferromagnetic behavior was obtained with several initial $MgCoO_{3-\delta}$ amounts, which are important for the selection of the correct dopant and concentration for application requirements.

4 Conclusion

A new solute solution of $(1\text{-}x)Bi_{0.5}Na_{0.5}TiO_3 + xMgCoO_{3-\delta}$ materials was fabricated using the simple sol–gel technique. The random incorporation of Mg and Co cations into the host lattice of the $Bi_{0.5}Na_{0.5}TiO_3$ materials during solution formation reduced the optical band gap values and induced a complex magnetic behavior. The optical band gap values of pure $Bi_{0.5}Na_{0.5}TiO_3$ materials were estimated to be approximately 3.05 eV and decreased to 2.22 eV for 9 mol% $MgCoO_{3-\delta}$ solution in the $Bi_{0.5}Na_{0.5}TiO_3$ compounds. The combination of diamagnetism and weak ferromagnetism was obtained for the pure $Bi_{0.5}Na_{0.5}TiO_3$ materials. The addition of $MgCoO_{3-\delta}$ to the host $Bi_{0.5}Na_{0.5}TiO_3$ materials as solid solution was resulted to suppress the diamagnetic component and induced the ferromagnetic ordering. The paramagnetic and/or antiferromagnetic-like behavior strongly influenced the ferromagnetism of typical $Bi_{0.5}Na_{0.5}TiO_3$ materials when $MgCoO_{3-\delta}$ was increased to over 5 mol%. The complex magnetic behavior of the $MgCoO_{3-\delta}$-modified $Bi_{0.5}Na_{0.5}TiO_3$ materials possibly resulted from the complex interaction of Co and Ti cations through O vacancies. We expect our work to be important in enhancing the magnetic performance of lead-free ferroelectric materials in the current development of green multiferroic materials.

Funding Information This research is funded by the Hanoi University of Science and Technology (HUST) under project number T2018-TĐ-201.

References

1. Quan, N.D., Bac, L.H., Thiet, D.V., Hung, V.N., Dung, D.D.: Adv. Mater. Sci. Eng. **2014**, 365391 (2014)
2. Smolensky, G.A., Isupov, V.A., Agranovskaya, A.I., Krainic, N.N.: Fiz. Tverd. Tela. **2**, 2982–2985 (1960)
3. Naderer, M., Kainz, T., Schutz, D., Reichmann, K., European Ceram, J.: Soc. **34**, 663–667 (2014)
4. Sung, Y.S., Kim, J.M., Cho, J.H., Song, T.K., Kim, M.H., Chong, H.H., Park, T.G., Do, D., Kim, S.S.: Appl. Phys. Lett. **96**, 022901 (2010)
5. Sung, Y.S., Kim, J.M., Cho, J.H., Song, T.K., Kim, M.H., Park, T.G.: Appl. Phys. Lett. **98**, 012902 (2011)
6. Ju, L., Shi, C., Sun, L., Zhang, Y., Qin, H., Hu, J.: J. Appl. Phys. **116**, 083909 (2014)
7. Thanh, L.T.H., Doan, N.B., Dung, N.Q., Cuong, L.V., Bac, L.H., Duc, N.A., Bao, P.Q., Dung, D.D.: J. Electron. Mater. **46**, 3367–3372 (2017)
8. Zhang, Y., Hu, J., Gao, F., Liu, H., Qin, H.: Comput. Theor. Chem. **967**, 284–288 (2011)
9. Wang, Y., Xu, G., Yang, L., Ren, Z., Wei, X., Weng, W.: Mater. Sci. Polan. **27**, 471–476 (2009)
10. Wang, Y., Xu, G., Ji, X., Ren, Z., Weng, W., Du, P., Shen, G., Han, G., Alloy, J.: Compound. **475**, L25–L30 (2009)

11. Thanh, L.T.H., Doan, N.B., Bac, L.H., Thiet, D.V., Cho, S., Bao, P.Q., Dung, D.D.: Mater. Lett. **186**, 239–242 (2017)
12. Dung, D.D., Doan, N.B., Dung, N.Q., Bac, L.H., Linh, N.H., Thanh, L.T.H., Thiet, D.V., Trung, N.N., Khang, N.C., Trung, T.V., Duc, N.V.: J. Sci. Adv. Mater. Dev. **4**, 584–590 (2019)
13. Dung, D.D., Doan, N.B., Dung, N.Q., Linh, N.H., Bac, L.H., Thanh, L.T.H., Trung, N.N., Duc, N.V., Cuong, L.V., Thiet, D.V., Cho, S., Supercond, J.: Novel Magn. **32**, 3011–3018 (2019)
14. Hue, M.M., Dung, N.Q., Phuong, L.T.K., Trung, N.N., Duc, N.V., Bac, L.H., Dung, D.D.: J. Magn. Magn. Mater. **471**, 164–168 (2019)
15. Hue, M.M., Dung, N.Q., Trung, N.N., Bac, L.H., Phuong, L.T.K., Duc, N.V., Dung, D.D.: Appl. Phys. A Mater. Sci. Process. **124**, 588 (2018)
16. Hung, N.T., Bac, L.H., Hoang, N.T., Vinh, P.V., Trung, N.N., Dung, D.D.: Physica B. **531**, 75–78 (2018)
17. Dung, D.D., Hung, N.T., Odkhuu, D.: Appl. Phys. A Mater. Sci. Process. **125**, 465 (2019)
18. Liu, X., Fan, H., Shi, J., Wang, L., Du, H.: RSC Adv. **6**, 30623–30627 (2016)
19. Tuan, N.H., Anh, V.K., Doan, N.B., Bac, L.H., Dung, D.D., Odkhuu, D., Sol-gel Sci, J.: Tech. **87**, 528–536 (2018)
20. Dung, D.D., Hung, N.T., Odkhuu, D.: J. Magn. Magn. Mater. **482**, 31–37 (2019)
21. Hung, N.T., Bac, L.H., Trung, N.N., Hoang, N.T., Vinh, P.V., Dung, D.D.: J. Magn. Magn. Mater. **451**, 183–186 (2018)
22. Shannon, R.D.: Acta Cryst. A. **32**, 751–767 (1976)
23. Chatzichristodoulou, C., Norby, P., Hendriksen, P.V., Mogensen, M.B.: J. Electroceram. **34**, 100 (2015)
24. Schmitt, V., Raether, F., European Ceram, J.: Soc. **34**, 15–21 (2014)
25. Niranjan, M.K., Karthik, T., Asthana, S., Pan, J., Waghmare, U.V.: J. Appl. Phys. **113**, 194106 (2013)
26. Zhu, J., Zhang, J., Jiang, K., Zhang, H., Hu, Z., Luo, H., Chu, J.: J. Am. Ceram. Soc. **99**, 2408–2414 (2016)
27. Domenico Jr., M.D., Wemple, S.H., Porto, S.P.S., Buman, P.R.: P.R., Phys. Rev. **174**, 522–530 (1968)
28. Sczancoski, J.C., Cavalcante, L.S., Badapanda, T., Rout, S.K., Panigrahi, S., Mastelaro, V.R., Varela, J.A., Li, M.S., Longo, E.: Powders. Solid State Sci. **12**, 1160–1167 (2010)
29. Barick, B.K., Mishra, K.K., Arora, A.K., Choudhary, R.N.P., Pradhan, D.K.: J. Phys. D. Appl. Phys. **44**, 355402 (2011)
30. Baedi, J., Mircholi, F., Moghadam, H.G.: Optik. **126**, 1505–1509 (2015)
31. Baedi, J., Mircholi, F.: Optik. **127**, 1503–1506 (2016)
32. Wood, D.L., Tauc, J.: Phys. Rev. B. **5**, 3144 (1972)
33. Thanh, L.T.H., Tuan, N.H., Bac, L.H., Dung, D.D., Bao, P.Q.: Commun. Phys. **26**, 51 (2016)
34. Phuong, L.T.K., Dung, D.D., Dung, N.Q., Hue, M.M., Duong, N.X., Luong, P.D., Bac, L.H., Duc, N.A., Trung, N.N., Duc, N.V., Odkhuu, D.: Mater. Res. Express. **6**, 106112 (2019)

Publisher's Note Springer Nature remains neutral with regard to jurisdictional claims in published maps and institutional affiliations.